[Frontiers in Bioscience, Landmark, 18, 224-240, January 1, 2013]

Single-molecule and bulk approaches to the DnaB replication fork helicase

Daniel L. Kaplan[1], Omar A. Saleh[2], Noah Ribeck[3]

[1]Department of Biological Sciences, Vanderbilt University, VU Station B, Box 35-1634, Nashville TN 37235, [2]Materials Dept., University of California, Santa Barbara CA 93106, [3]Department of Microbiology and Molecular Genetics, Michigan State University, 2215 Biomedical Physical Sciences, East Lansing MI 48824

TABLE OF CONTENTS

1. ABSTRACT

Motor proteins are enzymes that accomplish mechanical work in a wide variety of biological processes. In this review we focus on bulk and single molecule methods to study how motor proteins function. We discuss in detail the analysis of the motor protein DnaB, a hexameric helicase that unwinds DNA at a replication fork in Gram-negative bacteria. Bulk and single-molecule studies have complemented one another to arrive at a comprehensive mechanistic view of how DnaB unwinds double-stranded DNA.

2. INTRODUCTION

Motor proteins are enzymes that catalyze the conversion of chemical energy into mechanical work. They are among the most specialized and complex types of biomolecules that have evolved, as can be judged by our inability to build purely synthetic motor-protein analogs. Motor protein activity underlies a huge range of biological processes, including the workings of large-scale musculature; the growth, division, and movement of cells; and the replication, transcription, and translation of the genetic code.

Experimental study of these fascinating molecules has historically been somewhat hampered by their relative lack of an enzymatic product. Unlike an enzyme whose primary product is a long-lived (and therefore easily assayed) covalent modification, the primary product of a motor protein is a transient mechanical effect, such as a pulse of force or a nanometer-scale displacement. Of course, many motor proteins are powered by nucleotide hydrolysis, which is indeed a long-lived covalent modification that can be quantified relatively simply. However, such a measurement does not give any information on the mechanical output of the motor.

A more modern approach is to directly sense the forces generated by a motor, and/or the distances it transverses. Since such spatial and dynamic effects are transient (typically lasting of order milliseconds to seconds), their measurement requires an approach with high temporal resolution. Also, since motor proteins are only a few nanometers in size, the spatial and dynamic effects themselves are quite small—typical values are, respectively, a few tens of nanometers, and a few piconewtons. Thus, the measurement approach requires very high spatial/dynamic sensitivity. Further, the stochastic nature of motor proteins precludes synchronization of their activity, so it is not possible to amplify the spatial/ dynamic output by measuring many motors simultaneously. Finally, all of this must be done in solution, at room temperature, meaning that thermal fluctuations and Brownian motion are highly-significant barriers to acquiring high-resolution data. These requirements constrain the measurement approach to sensing one motor at a time. Generally, the study of single-molecules using applied force is termed single-molecule manipulation (SMM).

In this review, we generally discuss methods that can be used to study motor proteins using single-molecule manipulation (SMM) methods. Then, in order to compare and contrast the various motor-protein assays available, we review the assays used to study DnaB, a hexameric replicative helicase that has been subject to nearly all tracking methods available.

3. REVIEW OF SINGLE-MOLECULE MANIPULATION APPROACHES TO MOTOR PROTEINS

3.1. SMM Instrumentation

Single-molecule motor protein measurements can be accomplished by optical techniques, such as direct microscopic tracking of a fluorescent molecule attached to the motor, or by measuring the emission of multiple dyes that have a distance-dependent interaction. Here, we focus on an alternate approach: application of force, and real-time measurement of extension, of single biomolecules. Applying an external stress has enormous benefits in resolution: nearly all systems stiffen under an external load, so that the spring constant governing the system increases. The thermally-actuated fluctuations of a spring decrease as the spring constant increases—thus, application of an external force reduces the noise in single-molecule measurements, permitting sensing of minute changes in motor position. Further, force-application itself is done by attaching the biomolecule of interest to a micron-scale probe; since such a probe is large enough to efficiently scatter light, the measurement apparatus has no need to integrate a small optical signal for long periods of time, and the probe position can be tracked with high temporal resolution.

As a specific example, we consider a particular single-molecule apparatus, the magnetic tweezers. The magnetic tweezers (MT) is an instrument that utilizes an external magnetic field to stretch a DNA molecule that tethers a magnetic colloid to a glass surface (Figure 1). Biomolecular extension is measured, typically at rates of 60-200 Hz, by estimating the bead's position from its image, as captured by an inverted-light microscope (1, 2). In a typical setup, the magnetic field is generated by rare-earth magnets located above the sample, and force is controlled by varying the magnet/sample separation distance using computer-controlled motors. The force is not predicted from the field geometry, but rather calibrated by modeling the measured lateral motions of each tethered bead as a Brownian-actuated harmonic oscillator (3). Most simply, this can be done by computing the variance of bead position fluctuations in the direction of applied field, $\langle x^2 \rangle$, and applying the equipartition theorem of statistical mechanics, which estimates the force F to be

$$F = \frac{Lk_BT}{\langle x^2 \rangle},$$

where L is the bead height (tether length), and k_BT is the thermal energy. The equipartition approach is best used in the low-force limit, where the thermal bead fluctuations are large and thus easily measured; at higher forces, where parasitic noise can become comparable to the thermal fluctuations, a better estimate is found from comparing the power-spectrum of lateral fluctuations to those predicted from analysis of the Langevin equation (4, 5). For highest accuracy, this analysis must account for experimental limitations such as aliasing derived from the finite data-acquisition rate, unintentional low-pass filtering of the bead trajectory by the finite shutter time of the camera, and variations in the drag coefficient acting on the bead due to the proximity of the surface (1, 2, 6, 7, 8).

Compared to other single-molecule manipulation approaches (and particularly the optical trap), the MT is a simple yet versatile instrument. Force application and length measurement are achieved on a scale relevant to a single motor protein without the need for an extensive laser-based optical system. Further, the relatively uniform magnetic field creates a constant tension on the tethered DNA, which simplifies thermodynamic analysis of the resulting data, as the relevant potential is the Gibbs free energy, much like three-dimensional constant-pressure systems (9, 10, 11, 12). Historically, magnetic tweezers have had several drawbacks in comparison to optical traps, notably in their relatively low data-acquisition rate and

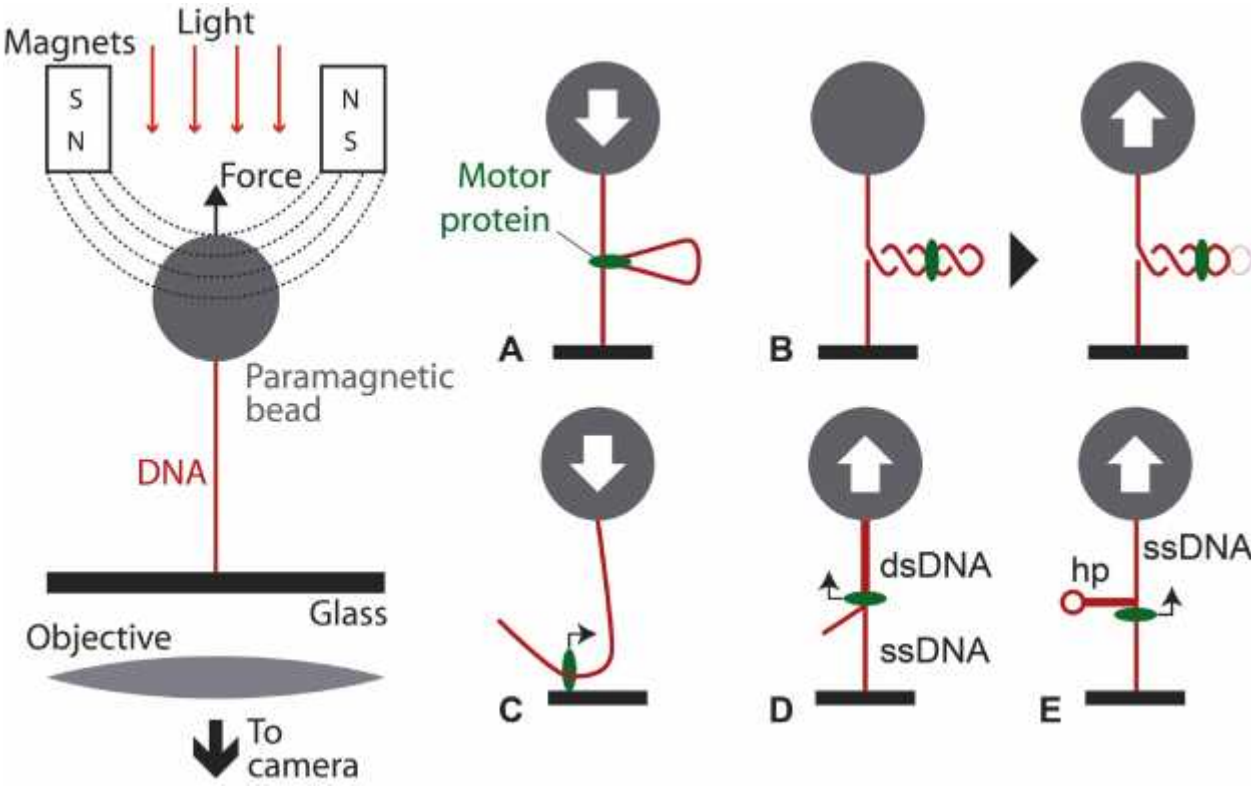

Figure 1. Left: Sketch of one SMM apparatus, the magnetic tweezers, in which a paramagnetic bead is tethered to a glass surface through a DNA molecule, and stretched with an external magnetic field. Bead position, and thus DNA length, is measured by microscopic imaging of the bead. (A-E) Various methods to transduce motor protein motion (direction indicated by small black arrows) into measurable changes in bead height (direction indicated by white arrows), including (A) loop formation by the motor; (B) changes in the number of plectonemes; (C) immobilization of the motor, and (D-E) conversion of dsDNA to ssDNA in two geometries (hp: hairpin).

limited resolution. However, recent technical advances have seen improvements in these areas, including kHz detection speeds (13), multiplexing (i.e. the ability to perform multiple experiments simultaneously) (1, 14); high spatial resolution tracking techniques (15); and methods to directly apply and sense torque (16, 17), which will enable the study DNA/protein interactions that have a rotational component, as with topoisomerases (18) and certain translocating motor proteins (19, 20).

3.2. Tether design for SMM

Each SMM measurement must be designed specifically for the motor protein to be studied. The geometry of the biomolecular complex that tethers and immobilizes the micron-scale probe must be designed such that the activity of the motor protein results in a measurable change in the tethered biomolecule.

DNA-based motor proteins are ideal candidates for study using SMM methods. Double-stranded DNA (dsDNA) is an optimal substrate biomolecule for multiple reasons: it is straightforward to synthesize large quantities of dsDNA through PCR or plasmid preps; immobilization labels can be added relatively easily using a variety of enzymatic methods (including, with PCR, the use of labeled primers); and dsDNA's non-reactive and hydrophilic nature causes few problems of non-specific adhesion. Using a simple dsDNA tether can be somewhat limiting, as it only works in the case that the activity of the motor of interest directly affects dsDNA extension. However, the ease of application has led to a relatively large number of studies that use dsDNA tethers to measure, for example, motors that spontaneously create loops of DNA that directly affect the measured probe height (Fig 1A) (20, 21, 22), and others that induce measurable rotation of the attached bead (23).

A powerful approach for motor proteins that modulate DNA twist is the plectoneme assay, in which, prior to introducing the motor, the dsDNA is twisted past the buckling point to form plectonemic loops. Twisting dsDNA requires that it be multiply labeled on both the 5' and 3' termini, since a single label permits free rotation, and thus would immediately relieve any torsional stress in the molecule. Creating multiple labels is a bit more difficult, as it implies adding labels internally to the DNA, rather than simply at the 5' or 3' termini (24). However, once such a tether is formed and twisted, any motor activity that changes the DNA twist will then create or destroy the plectonemic loops, affecting bead height (Figure 1B). This is a powerful approach because (i) the large size of a single plectonemic loop (~50-75 nm) (3, 25) means that small

twist changes (even less than a single turn) can be sensed, and (ii) dsDNA's helical nature causes many protein/DNA interactions to change the DNA twist. Plectoneme assays were originally designed to sense topoisomerase activity (18), and have been widely used in that regard (26, 27, 28, 29, 30). But, due to their sensitivity, these assays have also been used to sense more delicate interactions, such as the twist induced by a motor protein as it moves linearly along a DNA molecule (19), and the twist induced by local melting of the DNA upon binding of RNA polymerase (31).

A downside to plectoneme assays is that they are limited to relatively small applied forces, as larger forces pull the loops out, causing the DNA to undergo a variety of phase transitions (3, 32) and precluding measurements of motors. Since higher forces lead to higher-resolution measurements, this means that plectoneme assays are intrinsically of limited resolution, meaning that events of limited duration and/or distance cannot be measured. If it is necessary to perform high-resolution measurements of the linear translocation of a motor protein, then the optimal approach is to directly immobilize the motor itself. This geometry is sketched in Figure 1C; the idea is to immobilize the motor on one surface, the DNA substrate on the other, and to connect the two through the motor's intrinsic DNA binding activity. This is a difficult approach from a biochemical point of view, as it requires labeling and immobilizing the protein in such a way that its activity is not affected. However, it has been successfully carried out on a variety of proteins, including the phage φ29 DNA packaging motor (33), RNA polymerase (34), and the helicase RecBCD (35). In this assay, the limit on resolution ultimately derives from the motor itself: large enough forces tend to stop ('stall') motors. This means a higher-resolution measurement can be made on a stronger motor than a weaker one; so, for example, individual sub-nanometer steps have only been measured for strong motors such as RNA polymerase and the phage packaging motor.

A final strategy is to design DNA molecules with complex secondary structure aimed at a particular class of motors. So, for example, motors involved in processing Holliday junctions can be measured by assembling DNA strands into a cruciform structure that is used to tether the probe (36, 37). The most common application of secondary-structure design is in the study of helicases (Figs. 1D,E), likely the largest class of DNA-based motor proteins. Helicases are motors that catalyze the separation of dsDNA into two component single-strands (ssDNAs). In general, this is not a permanent change, as the ssDNAs can reform inter-strand basepairs after the helicase has passed. Special considerations are thus needed when studying isolated helicases in bulk, as discussed in Section 3. However, in the SMM experiments, mechanical force can be used to keep the ssDNAs apart from each other. Further, the conversion of dsDNA to ssDNA offers a variety of strategies to measure helicase activity. We discuss this at length below in our discussion of the helicase DnaB.

4. COMPARING AND CONTRASTING BULK AND SMM MEASUREMENTS OF THE HELICASE DNAB

4.1. Bulk characterization of DnaB

4.1.1. Purification and Initial Characterization of E. coli DnaB

E. coli DnaB was originally over-expressed, purified, and characterized in bulk solution (38). SDS/PAGE revealed that the protein is ~ 48 kDa, gel filtration and sedimentation experiments revealed that this protein forms a hexamer in solution, and this was consistent with protein crosslinking experiments with dimethyl suberimadate (38). Analytical centrifugation of purified *E. coli* DnaB was later accomplished, confirming that DnaB formed a hexamer in solution in a manner dependent on magnesium (39). DnaB exhibits ssDNA-dependent ATPase activity that requires magnesium (40).

DnaB was later crystallized in solution, yielding high purity protein (41). With highly purified DnaB, nitrocellulose filter binding was used to show that DnaB binds to single or double-stranded DNA (42). Equilibrium gel filtration was then used to show that DnaB binds one ATP molecule per protomer (43). Gel filtration was also used to show that DnaB requires ATP or ATP- S to bind stably to ssDNA (43). It was also established using DnaB, *E. coli* primase, and ssDNA that DnaB can stimulate the ability of primase to synthesize RNA primers using ssDNA as a template (44, 45).

4.1.2. It is established that DnaB is a helicase using purified protein and radiolabeled DNA

A major breakthrough in the understanding of DnaB mechanism came it was discovered that DnaB is a DNA helicase (46). A radiolabeled oligonucleotide was annealed to M13 ssDNA and incubated with DnaB and ATP, and the results were analyzed by native agarose gel electrophoresis (46). The results show that DnaB unwinds DNA (46). To confirm that the unwinding was due to DnaB, it was shown that the unwinding activity (1) requires a hydrolyzable ribonucleoside triphosphate, (2) is inhibited by antibody against DnaB, and (3) is inhibited by prior coating of the ssDNA with single-stranded binding protein (46). It was also shown that DnaB requires the presence of both 5' and 3' single-strand extensions attached to the end of the duplex (46).

4.1.3. Domain function of DnaB is elucidated

The role of different domains of DnaB on mechanism was then dissected (47). It was found that the C-terminal domain can form hexamers, while the N-terminal domain formed dimers (47). A region of DnaB was identified that hydrolyzes ATP (47). This work was followed by data demonstrating that the C-terminal domain binds DNA (48). Site-directed mutagenesis was also performed to identify residues of DnaB involved in multimerization, DNA binding, and ATPase activity (48).

4.1.4. Fluorescent studies demonstrate that DnaB binds to 20 nucleotides of ssDNA

A fluorescent analog of DNA was used to measure the DnaB site size on ssDNA (49). It was found

that DnaB binds polymer ssDNA with a site size of 20 nucleotides per protein hexamer (49). Photo-crosslinking was also used to show that the DNA only contacts one of the DnaB protomers (49). The possibility that ssDNA wraps around the DnaB hexamer was excluded in these studies (49). Fluorescence was also used to determine that DnaB binds tightly to ssDNA in the presence of ATP- S (50). The kinetics of ssDNA binding by DnaB was also investigated using stop-flow kinetics (51). It was found that a 10-mer bound to a strong ssDNA binding subsite of DnaB, and the kinetics also revelead at least three enzymatic steps for ssDNA binding by DnaB (51).

Several years later, the binding of DnaB to a physiologically-relevant DNA forked structure was examined (52). The techniques of fluorescence titration, fluorescence energy-transfer, and analytical ultracentrifugation were used to show that dsDNA does not contribute to the affinity of DnaB for the forked-structure, suggesting that interaction of DnaB with forked-DNA is mediated through ssDNA interactions (52). Furthermore, the data showed that one hexamer of DnaB interacts with the 5'-single-strand extension, and a second hexamer of DnaB interacts with the 3'-single-strand extension (52). The two hexamers are bound in opposite orientations with respect to the dsDNA (52). The helicase domain is adjacent to the duplex on the relevant 5'-single-strand extension (52).

4.1.5. Rapid quench flow technique reveals mechanism of ATP hydrolysis

The mechanism of ATP binding and hydrolysis catalyzed by DnaB was examined in several studies (53, 54, 55). ATP binding was explored using fluorescent analogs of ATP, and the data showed a minimum of four steps for ATP binding (53). When ATP hydrolysis was examined, it was found that all six subunits of DnaB are active in hydrolyzing ATP (54). Recently, the rapid quench-flow technique was used to explore the effect of ssDNA on NTP hydrolysis (55). The kinetics of NTP hydrolysis were affected by the type of nucleotide cofactor and the base composition of DNA (55). The effect of DNA on the NTP hydrolysis rate derives from the strong ssDNA binding site on DnaB, and the function of the weak ssDNA binding site is to modulate the effect of the strong ssDNA binding site (55).

4.1.6. Electron microscopy shows that single-stranded DNA passes through the central channel of T7 gp4

A breakthrough in the mechanism of hexameric helicase activity came with studies of the DnaB-related protein, T7 gp4. Using electron microscopy, it was shown that T7 gp4 forms a hexamer that encircles ssDNA (56, 57)_ENREF_10. The authors synthesized this information with previous data showing that T7 gp4 requires a forked-shaped duplex for unwinding (58). There was also an important paper that showed that T7 gp4 unwinding was inhibited when a DNA adduct was attached to the strand bearing the 5' single-strand extension, but not the complementary strand (59). Based on these sets of data, the authors proposed that one DNA strand passes through the central channel of T7 gp4, while the other DNA strand passes outside the ring (56, 57)_ENREF_11_ENREF_11.

4.1.7. Fluorescent energy transfer show that single-stranded DNA passes through the central channel of DnaB

To address whether DnaB encircles single-stranded DNA in solution, fluorescence energy transfer was employed (60). A fluorescent donor was placed on DnaB, and a fluorescent acceptor was placed on various positions of the DNA (60). Using fluorescence information from multiple donor-acceptors, the group concluded that ssDNA passes through the central channel of DnaB (60). This work is the first to demonstrate that DnaB encircles single-stranded DNA, and it is also the first to show that a hexameric helicase encircles ssDNA in solution (60).

4.1.8. Fluorescence studies reveal kinetics of DnaB-catalyzed unwinding

Kinetics of DnaB unwinding double-stranded DNA were analyzed by the quench flow technique (61). These studies revealed a number of interesting properties of the DnaB-catalyzed unwinding mechanism, including that the number of base pairs unwound in a single catalytic step is 1.4 (61). Furthermore, the catalytic speed was measured at 291 bp/sec (61). The rapid quench flow technique was used to show that the 3'-single-strand extension controls the unwinding rate and processivity of the helicase (62). These data led to the conclusion that the helicase transiently interacts with the strand bearing the 3'-single-strand extension during unwinding (62). It was also shown that the GC-content of the dsDNA has a large effect on the unwinding activity of the enzyme (62).

4.1.9. Electron microscopy studies of DnaB reveal its shape

Using electron microscopy images of negatively stained DnaB, a three-dimensional reconstruction of the protein hexamer at 27 angstroms resolution was produced (63). A central channel was clearly visible, and the DnaB exhibited three-fold symmetry. Three-dimensional cryo electron microscopy was performed several years later (64). The hexamer displayed two faces, one with three-fold symmetry and one with six-fold symmetry (64, 65)_ENREF_31. Several years later, a follow-up electron microscopy study demonstrated that the N-terminal domain makes two different contacts with neighboring subunits, while the helicase domain exists in two alternate conformations (66).

4.1.10.Crystal structures of T7 gp4 and DnaB reveal information about helicase mechanism

The first crystal structure of T7 gp4 helicase domain revealed a helical filament that resembles RecA (67). Furthermore, a conserved arginine residue contacts the gamma phosphate of the nucleotide in *trans* (67). This arginine is important for hydrolysis of ATP, and it has been referred to as the "arginine finger". The following year, a structure of the T7 gp4 helicase domain formed the physiologically relevant ring-shape (68). The structure was not six-fold symmetric, and four of the six protomers showed binding to AMP-PNP (68). Furthermore, the domain that crystallized was shown to be active as a helicase in solution. These data suggested a "binding-change mechanism" for the sequential hydrolysis of ATP

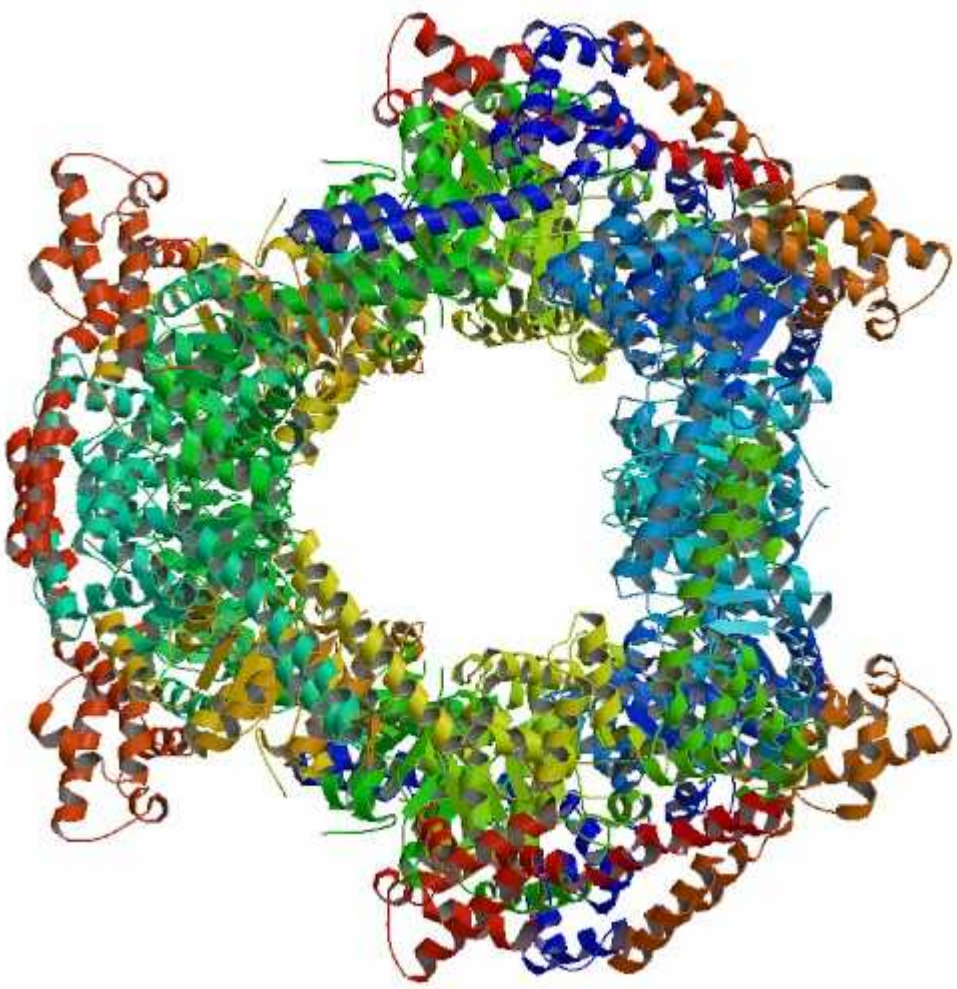

Figure 2. Crystal structure of *Bacillus stearothermophilus* hexameric DnaB in complex with a domain of DnaG primase, from crystal structure coordinates deposited from (73).

by gp4 in solution (68). Several years later, a crystal structure of the helicase-primase protein T7 gp4 crystallized as a heptamer, and the structure was determined at 3.45 angstroms resolution (69). The heptamer formed showed a great degree of flexibility between the helicase and primase domains, suggesting how DNA unwinding is coupled to primer synthesis (69).

Crystal and NMR structures of the N-terminal region of DnaB revealed that the domain was highly helical and globular (70, 71)_ENREF_36. The first crystal structure of full-length DnaB was from *Thermus aquaticus*, and it crystallized as a monomer (72). The C-terminal domain exhibited a classic RecA fold, while the N-terminus contained a helical hairpin (72). The authors compared the structure to that of the papilloma virus E1 protein, and concluded that the two helicases unwind DNA by different mechanisms (72). Later that year, the hexameric structure of DnaB from *Bacillus stearothermophilus* was determined (73). The structure showed that the N-terminal domains pack into a triangular collar seated on top of a packed ring of C-terminal domains (73) (Figure 2). The six N-terminal domains form a trimer of head-to-head dimers (73) (Figure 2). The diameter of the central channel of the N-terminal domain is ~ 50 angstroms, while the diameters of the central channel of the C-terminal domains varies from ~25 angstroms to ~50 angstroms (73) (Figure 2). Thus, the diameter of the central channel is very dynamic and capable of accommodating double-stranded DNA (73). The crystal structure of the DnaB-related protein G40P was also determined (74). The structure revealed that the N-terminal domain is three-fold symmetric, while the C-terminal domain is six-fold symmetric (74).

4.1.11. My (Kaplan) studies of DnaB

Purification methods for *E. coli* and *T. aquaticus* DnaB are described in detail elsewhere (75, 76). One advantage to studying *T. aquaticus* DnaB is that the protein is heat-stable, and an initial heating step denatures many of the *E. coli* protein contaminants (77). The design of duplex DNA to monitor DNA unwinding catalyzed by DnaB is important. Many of the details have been described

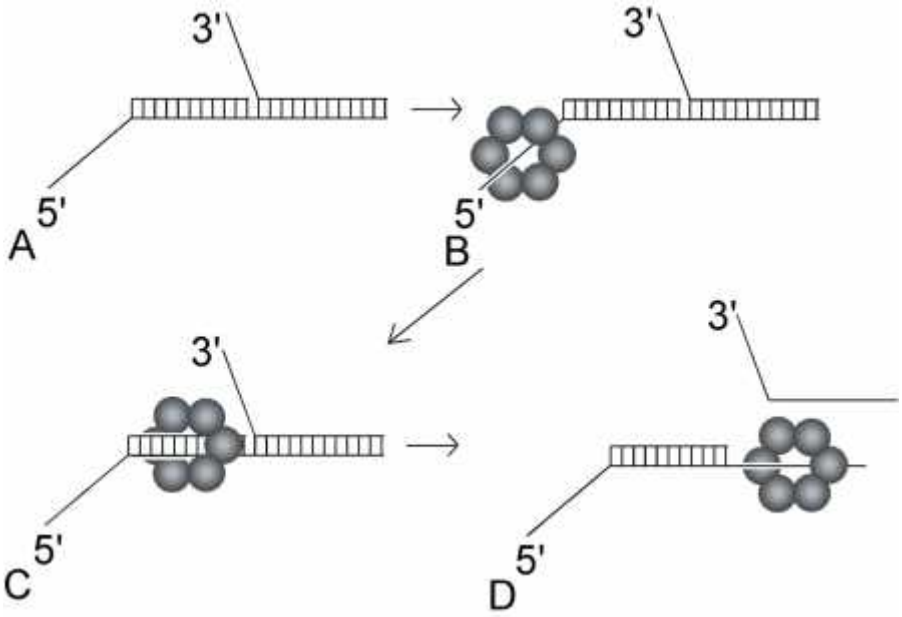

Figure 3. DnaB translocates along double-stranded DNA, and unwinds a forked-DNA structure positioned downstream of its loading site. (A) Substrate used to test DnaB translocation. (B) DnaB loads on the 5'-single-strand extension and moves in the 5' to 3' direction toward the duplex. (C) DnaB encircles two DNA strands and translocates toward the downstream duplex. (D) DnaB encircles one DNA strand to unwind the downstream duplex.

elsewhere (75). An important consideration is the annealing time of the DNA oligonucleotides used to form the duplex DNA substrate. If the strand-annealing rate is faster than the DnaB-catalyzed unwinding rate, no unwinding will be observed. To circumvent this potential problem, we (Kaplan and Steitz) use DNA oligonucleotides that have a slow annealing rate, with a half-time of annealing of approximately 1 to 2 hours. The sequence of the DNA duplex used to study *Thermus aquaticus* DnaB unwinding is published (77).

Most DNA helicases will not unwind blunt duplex DNA. A single-strand extension is generally required for unwinding, and the polarity of the single-strand extension generally defines the polarity of the helicase. For example, if the helicase requires a single-strand extension with a 3'-end to unwind the DNA, the helicase unwinds DNA with 3' to 5' polarity. Steitz and I initially observed that *T. aquaticus* DnaB requires 10 nucleotides of a 5' extension, and 30 nucleotides of a 3' single-strand extension for maximal DNA unwinding. Thus, the polarity could not be defined by the requirement for single-strand extensions. We then reversed the polarity of the 5' and 3' single-strand extensions and found that *T. aquaticus* DnaB can unwind DNA with two 5' extensions, but DnaB cannot unwind DNA with two 3' extensions (78). These data led us to conclude that *T. aquaticus* DnaB unwinds DNA with 5' to 3' polarity.

I next investigated why DnaB requires a 3' single-strand extension for maximal DNA unwinding. Chemical modifications to the 3'-single-strand extension had little effect on the unwinding rates observed (78). However, I found that with no 3'-single-strand extension, DnaB does not fail to move. In fact, DnaB encircles both strands when it encounters a duplex with no 3'-single-strand extension (78). DnaB continues to translocate along this duplex, and *DnaB* can unwind a DNA duplex that is positioned downstream (78) (Figure 3). These data suggest that the 3'-single-strand extension is a steric factor that determines whether one or two strand pass through the central channel of DnaB (78). I also concluded that DnaB unwinds DNA by a steric exclusion mechanism (78). The idea that DnaB can encircle two DNA strands was supported seven years later, when a crystal structure of hexameric DnaB from the Steitz lab reported a central channel of 50 angstroms (73).

Working with Mike O'Donnell, I next examined an important question. When DnaB is translocating along double-stranded DNA, does the helicase use the energy from NTP hydrolysis to unidirectionally move along the DNA, or slide along DNA in both directions without hydrolyzing NTP? To answer this question, we investigated whether *E. coli* DnaB can drive branch migration of Holliday junctions. In fact, we found that DnaB was very efficient in driving branch migration of Holliday junctions bearing a 5'-single-strand extension (79) (Figure 4). Furthermore, DnaB can dislodge proteins while translocating along dsDNA (79). Branch migration and protein displacement activities each required ATP, suggesting that DnaB can actively translocate along dsDNA (79). We also found that T7 gp4 can drive branch migration of Holliday junctions, suggesting that helicases related to DnaB can also actively translocate along dsDNA (79).

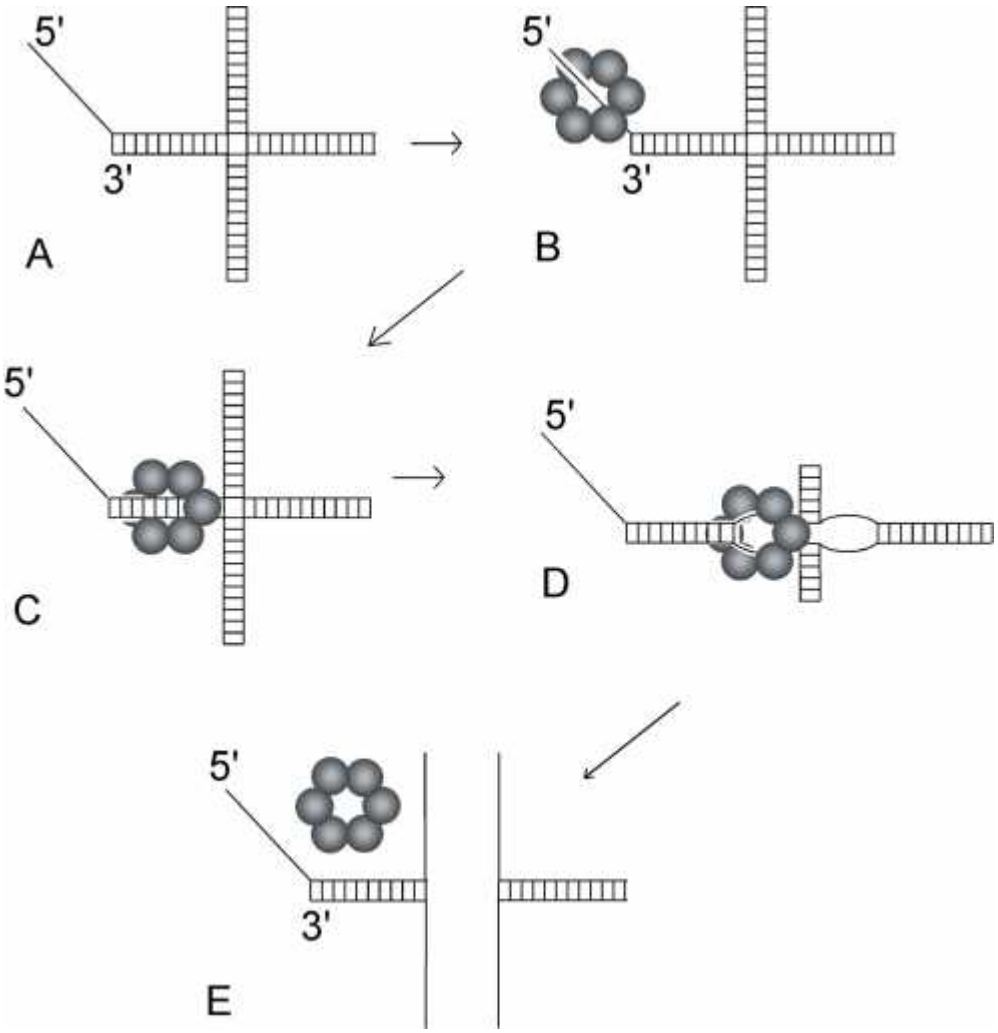

Figure 4. DnaB drives branch migration of a Holliday junction with a 5' single-strand extension. (A) Substrate used to test DnaB branch migration activity. (B) DnaB loads on the 5'-single-strand extension and moves toward the DNA duplex. (C) DnaB encircles two DNA strands and moves toward the branch point. (D) DnaB encircles two DNA stands and drives branch migration of the Holliday junction. (E) Branch migration is complete.

We also examined whether DnaB can unwind DNA if a Holliday junction bears a forked DNA structure. We found that DnaB was quite efficient in unwinding a Holliday junction if it bears a forked-DNA structure (79) (Figure 5). We found concentration dependent activation of DNA branch migration. Branch migration and unwinding activity was observed at DnaB concentrations as low as 6 nM (unpublished). As DnaB concentration was progressively increased from 6 nM to 19 nM, 60 nM, 180 nM, and 590 nM , there was a progressively higher fraction of product DNA (unpublished). Concentrations of DnaB above 590 nM were less efficient in driving branch migration (unpublished). A similar concentration dependence was observed for unwinding (unpublished). It may be that 6 nM is required to observe branch migration or unwinding because this is the concentration required to form hexameric DnaB (39). *It is important to emphasize that both branch migration and unwinding are observed at low (6 nM) concentrations of DnaB, suggesting that the hexameric form of DnaB catalyzes DNA branch migration and unwinding.*

We found that DnaB drives branch migration by encircling two DNA strands, and DnaB translocates along the DNA inside to drive unidirectional branch migration (79). We used biotin/streptavidin blocks to determine which DNA strands are passing through the central channel of DnaB (79). For unwinding, biotin/streptavidin only blocks activity when it is placed on one of the strands (79). In contrast, for branch migration, biotin/streptavidin blocks activity when it is placed on either of the two strands (79). We also reversed the polarity of the strands to examine the polarity of strand translocation (79). We found that during branch migration and unwinding, activity is blocked by reversing the polarity of the strand that bears the 5'-single-strand extension, but not any of the other strands (79).

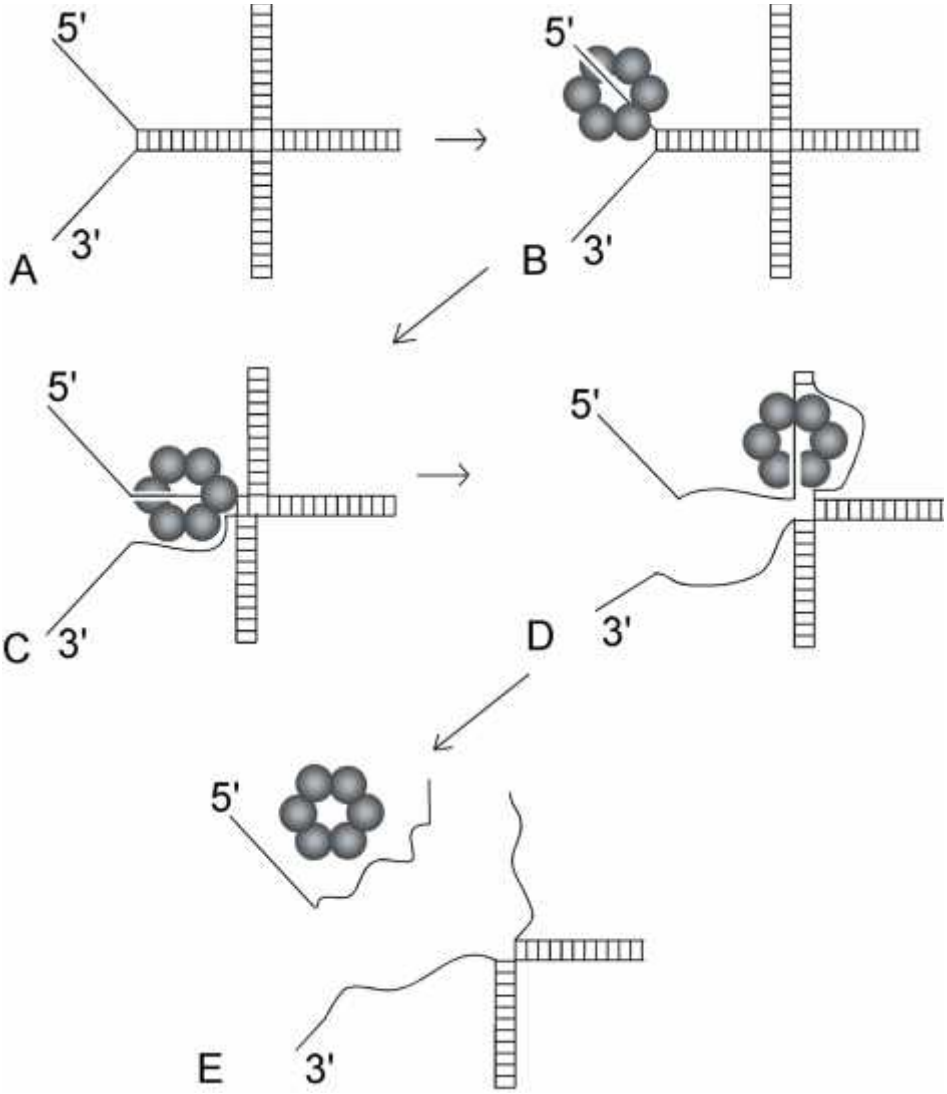

Figure 5. DnaB unwinds a Holliday junction with a forked-shaped extension. (A) Substrate used to test DnaB unwinding activity. (B) DnaB loads on the 5' single-strand extension and moves toward the DNA duplex. (C) DnaB encircles one DNA strand and unwinds the strand bearing the 5'-single-strand extension. (D) DnaB continues to unwind the strand bearing the 5'-single-strand extension. (E) The strand is unwound.

These data suggest that for either DNA unwinding or branch migration, DnaB functions by translocating along the strand bearing the 5'-single strand extension in the 5' to 3' direction (79).

We continued these studies with longer, heterologous Holliday junctions, and found that DnaB can drive branch migration of a long, heterologous Holliday junction if 5' single-strand extensions are placed on opposite sides of the junction (80). We also found that DnaB can encircle three strands if the protein encounters a third-strand during translocation (80). Finally, we concluded in this study that the DNA binding site is buried inside the central channel of DnaB (80). All of these conclusions were derived from observing DnaB activity on various assemblies of DNA strands (80).

4.1.12. DnaB functions with other proteins

This review has focused on the study of DnaB alone, functioning as a motor protein. In the cell, DnaB works in concert with Pol III, the replicative polymerase, and the tau subunit of Pol III acts as a connecting link between the replicative helicase and the replicative polymerase (81). Elegant experiments have been accomplished with DnaB acting in coordination with the Pol III (82, 83, 84). DnaB is also important for primase recruitment and action, and a direct interaction has been observed between DnaB and DnaG (primase) using pulldown methods and gel filtration (73, 85). The interaction between DnaG and DnaB has been reported to influence replication fork timing (86), and more recently interaction between DnaG and DnaB has been analyzed in detail (87). DnaB is loaded onto ssDNA with the

assistance of DnaA and DnaC, and numerous groups have worked to reveal the mechanism of this loading process (88, 89, 90, 91, 92, 93, 94). It has also been demonstrated that DnaG directs the release of DnaB from DnaC (89). Furthermore, it has been shown that DnaC modulates the activity of DnaB at Holliday junctions (95). There is also an elegant mechanism for reloading DnaB onto DNA in the case of DNA damage (96, 97). Furthermore, DnaB binds directly to rep, a second helicase at a replication fork (98, 99). Finally, the termination of DNA replication involves DnaB (100, 101, 102, 103). Future work will reveal how DnaB motor function is influenced by cellular partners. A recent study, for example, reveals that a repair polymerase can slow the speed of DnaB (104).

4.2. Single-molecule characterization of DnaB

To contrast with the bulk approaches just described, we now discuss our recent single-molecule work on DnaB (105). As mentioned previously, the unique abilities of helicases to modulate DNA secondary structure permits a different class of SMM experiment in which the tether is specifically designed to exploit the DNA denaturation activity of a helicase. For replicative helicases, the logical tether design is a simulacrum of the replication fork, with a duplex region terminating in two ssDNA strands (the 5' and 3' tails). Thus, the tether effectively has three extremities. An SMM measurement requires application of a force, which is (in static equilibrium) an intrinsically dipolar quantity, with two equal and opposite forces applied to different ends of the substrate. Thus, for SMM experiments on a forked substrate, there are three different possible geometries corresponding to the different ways to choose two mechanical attachment points from the three fork extremities. These three geometries are:

1) The hairpin geometry: force on the 5' and 3' tails. This geometry is widely studied (105, 106, 107, 108, 109, 110, 111), as it permits direct amplification of motor activity: each basepair opened in the duplex adds two bases to the extension of the tether (one to each tail). So, while the hairpin geometry is intrinsically limited to small forces (since forces greater than 15 pN mechanically denature the DNA), the amplification has permitted hairpin-based experiments to measure step sizes of helicases (111).

2 and 3) The 5' and 3' fork geometries: force on the duplex and either the 5' or 3' tail. This geometry relies on the differing extensions of dsDNA and ssDNA to measure helicase activity, rather than a change in the number of bases in the tether (as in the hairpin). Measuring helicase activity thus requires quantification of the force-extension relation of dsDNA and ssDNA, which can be done by single-molecule force-extension measurements (112, 113, 114). This type of differential-extension measurement was first used to measure polymerase activity, in which dsDNA is created from an existing ssDNA strand (115, 116), and was later applied to helicases (117). The assay is limited to relatively high forces, which create sufficient differential extension, as well as a kinetic barrier to strand reannealing. Further, the resolution of this assay is relatively low, as each base unwound increases the tether length by only a fraction of a nanometer (i.e. the difference between the high-force extensions of a dsDNA basepair, ~ 0.34 nm, and an ssDNA base, ~0.5nm). One notable exception to this is a low-force study (< 5 pN) which uses differential elasticity in the low-force regime to relate a decrease in extension to helicase activity. In this case, strand reannealing is prevented by flow (118).

In any SMM measurement of a motor protein, an important consideration is the effect of force on motor kinetics. Indeed, a large literature exists that discusses the effects of an external mechanical load on the translocation of a motor (119). In the case of helicases, the issue is more subtle and perhaps more interesting. In particular, the two issues that arise are i) the interplay between the DNA destabilization activity of the helicase and that of the applied force, and ii) the effects of force in modulating DNA/helicase interactions. Together, these two issues determine how the rate of helicase unwinding is affected by the external force.

A simple way to conceptualize the multiple roles of force in affecting helicase activity is shown in the sketch of DnaB on a fork, Figure 6. Each of the three extremities of the fork (the duplex, 5', and 3' tails) can affect DnaB activity, and force can modulate each of the three possible interactions described above. However, since force is a dipole, it will always be applied to (and possibly modulate) at least two of the interactions, leading to some indeterminacy in interpreting the results—upon measuring an effect of force on helicase geometry, it is unclear which, or both, of the two interactions were affected by force. Getting around this requires performing measurements in all three possible geometries, and performing pairwise comparisons of the results in order to isolate the different effects. The end result is a holistic, integrated view of the suite of interactions between the helicase and a DNA fork. These interactions can affect all aspects of helicase activity; for DnaB this specifically manifests in variation of both its unwinding velocity and tendency to pause. Here, for simplicity, we focus on the helicase's speed, and refer the reader to the original research paper (105) for the analysis of pausing, which is entirely consistent with the speed analysis.

First consider the activity of DnaB in the hairpin geometry. The helicase causes constant-velocity increases in bead height; using a model for ssDNA elasticity, this velocity can be translated into the unwinding velocity of the motor. This unwinding velocity varies strongly with the applied force, which can be attributed to the destabilizing effect of force on the DNA basepairs: at higher forces, the basepairs fluctuate open more frequently, allowing the helicase to open them more quickly. This type of behavior (where helicase velocity is highly dependent on basepair stability) is known as 'passive' helicase activity, after the suggestion of Lohman (120), and the more recent classification scheme of Manosas *et al.* (121); it can be contrasted with 'active' behavior of certain helicases in which the velocity is the same, regardless of basepair stability. Following the model of Betterton and Julicher (122, 123), it is possible to quantitatively model the passive nature of DnaB; the result is that DnaB's unwinding is

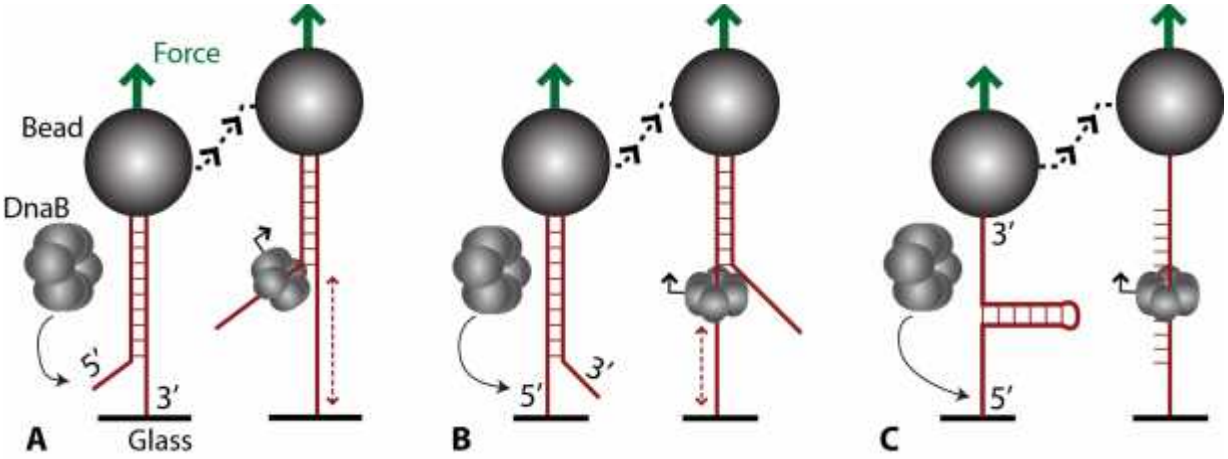

Figure 6. Different tether geometries for assaying DnaB helicase activity in an SMM experiment. (A) 3' fork geometry; (B) 5' fork geometry; (C) hairpin geometry.

close in behavior to a passive helicase, similar to other hexameric helicases that have been studied (106, 124).

Multiple SMM studies of helicases have used hairpin measurements to establish the active or passive nature of the helicase. However, our discussion above should make clear that the philosophy underlying this approach is flawed: it intrinsically assumes the only effect of force is in modulating dsDNA stability, with no effect on helicase/DNA interactions. We have experimentally demonstrated that such effects are important by comparing DnaB unwinding rates on the hairpin substrate with those on the 3' fork substrate (recall that the 3' fork involves applying force to the duplex and 3' tail, and not to the 5' tail onto which the helicase loads; see Figure 7). In the fork geometry, the duplex is loaded and thus destabilized; thus, the helicase velocity again increases with force. A complication is that the free energy of duplex destabilization is different when the same force is in the fork and hairpin geometries, so it is not appropriate to compare unwinding velocity in the two assays at equivalent forces. Instead, the appropriate comparison is to compare velocities between geometries at equal free energy of destabilization (10) (which is the key parameter in active/passive theories). Doing this essentially factors out the duplex destabilization, bringing into focus other differences between the geometries. And, indeed, they are different: DnaB is consistently faster in the 3' fork geometry than the hairpin geometry.

The origin of the velocity difference between hairpin and 3' fork substrate could be due to several factors. There are two immediate and obvious differences: first, in the hairpin the DnaB-bound strand is under tension, while it isn't in the 3' fork (so there could be a difference in how DnaB interacts with the bound strand); second, in the hairpin the two ssDNA tails are peeled apart, which is not the case in the 3' fork (so there could be a difference in how DnaB interacts with the occluded strand). However, a single point of comparison is not sufficient to differentiate the effects. Thus, a set of data in another geometry is needed; this is exactly what the 5' fork geometry gives. Experiments in the 5' fork geometry share aspects of each of the others: the DnaB-bound strand is under tension (like the hairpin, but not the 3' fork), while the ssDNA tails are not peeled apart (like the 3' fork, but not the hairpin).

Unwinding measurements in the 5' fork geometry show that DnaB's unwinding activity matches the 3' fork velocity at low forces (~20 pN), but is significantly slower at higher forces (> 30 pN). This resolves the indeterminacy: that the rate in the two fork assays matches at 20 pN indicates that tension on the bound strand does not affect activity for forces below 20 pN; thus, the hairpin/3' fork difference cannot be attributed to the bound-strand tension, and instead must be attributed to the peeling effect. Indeed, bulk results (discussed above) have suggested that DnaB has an activating interaction with the occluded strand (125), which is consistent with the conclusion that mechanically peeling the occluded strand away from DnaB slows the helicase. However, the high-force 3'/5' difference can indeed by attributed to the effect of force on the bound state; indeed, quantitative models of the effect of force on DnaB translocation can correctly predict the ratio of velocities, assuming a reasonable step size of 1 basepair.

We summarize this section by discussing the SMM measurements of DnaB in the context of the recent active/passive framework proposed by Manosas *et al.* (121). In that work, the authors argued that the active/passive classification cannot and should not be applied completely within the confines of a quantitative model, as the system complexity precludes a one-to-one relationship between the relatively few measured parameters and the large number of unmeasured, but possibly important, system parameters. Most models (notably, that of Betterton and Julicher (122, 123)) predict the unwinding rate as a function of an 'active' parameter, describing the propensity of the helicase to destabilize DNA, along with the intrinsic DNA stability (itself a function of DNA sequence and applied force). Manosas *et al.* argue that, unless certain variables are known (e.g. the

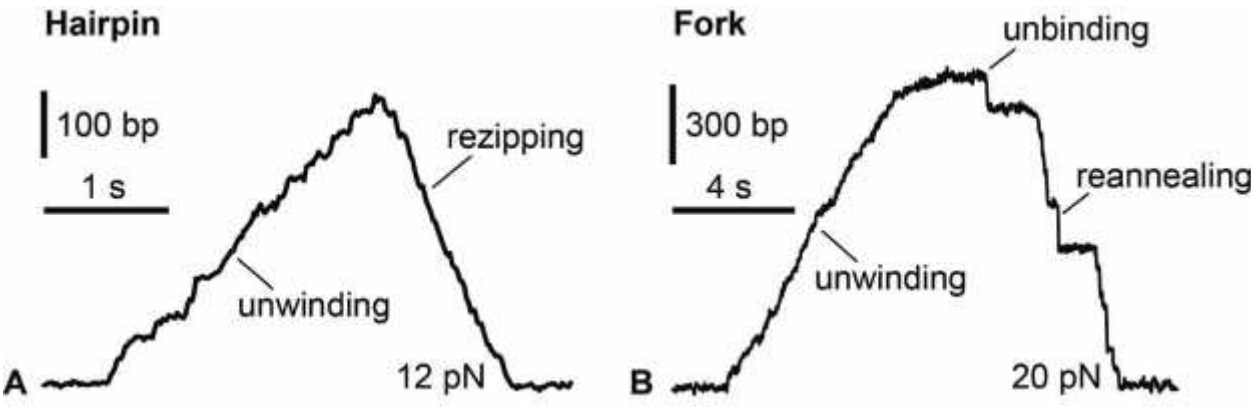

Figure 7. Typical single-molecule measurements of helicase activity in (A) the hairpin geometry, and (B) the 3' fork geometry. In both cases, unwinding increases the measured bead height. The differing geometries affect the unwinding rate and pausing tendency. Event recoveries also differ, as DnaB translocates around the hairpin, permitting continuous rezipping, whereas DnaB unbinds from the fork, and the DNA stochastically reanneals.

helicase's backwards stepping rate, or its step size), different sets of parameters can yield nearly identical quantitative predictions of unwinding activity. Our work on DnaB serves to illustrate and reinforce the point of Manosas—we have shown that the geometry of applied force is yet another variable that can affect unwinding rate, and that is typically not directly controlled for in most experiments. Finally, while this discussion centers specifically on the activity of helicases, we note that the effects of force in many motor protein measurements might be similarly nuanced.

5. SUMMARY AND PERSPECTIVE

We have discussed general issues of motor protein measurement, and illustrated that discussion with specific remarks on bulk and single-molecule measurements of DnaB. What we hope is clear from the DnaB discussion is the progressive nature of our understanding of DnaB's structure and mechanism: starting from basic biochemical measurements (such as measurements of the size of the DnaB complex), progressing to more subtle and directed assays that investigated DnaB's quaternary structure, its orientation within a DNA fork, and its direction of translocation. Given those results of bulk biochemistry, it became possible to design and interpret single-molecule assays that answered fundamental questions of microscopic mechanism, including important details about DnaB's interactions with basepairs and the bound ssDNA strand.

Extrapolating from work on DnaB, we can make some basic predictions on future developments in motor protein work. First, for DnaB in particular, we expect single-molecule studies to mature and become more complex, focusing on, e.g., interactions with other replisome components, just as has occurred in for bulk studies. Second, the study of other motors will mature, and become advanced enough to permit single-molecule approaches. The eukaryotic analog to DnaB, the MCM complex, is a prime example of this, as basic identification of the composition of the eukaryotic replicative helicase is now occurring. Finally, on the instrumental front, a clear direction for future development is the marriage of high-resolution single-molecule manipulation approaches with the local information derived from tracking fluorescent dyes attached to the motors; indeed, devices that accomplish this combination have begun to appear (126, 127). For DnaB, for example, such a study could clarify exactly where the occluded strand is located, and how it helps activate the helicase.

6. ACKNOWLEDGEMENTS

All authors contributed equally to this article. O.A.S. and N.R. acknowledge support from the National Science Foundation under grant No. PHY-0748564. D.L.K. acknowledges support from American Cancer Society Research Scholar Grant #RSG-08-124-01-CCG.

7. REFERENCES

1. N. Ribeck and O. A. Saleh: Multiplexed single-molecule measurements with magnetic tweezers. *Rev. Sci. Instrum.*, 79(9), 094301-6 (2008)

2. C. Gosse and V. Croquette: Magnetic Tweezers: Micromanipulation and Force Measurement at the Molecular Level. *Biophys. J.*, 82(6), 3314-3329 (2002)

3. T. R. Strick, J.-F. Allemand, D. Bensimon, A. Bensimon and V. Croquette: The elasticity of a single supercoiled DNA molecule. *Science*, 271(5257), 1835-1837 (1996)

4. S. F. Norrelykke and H. Flyvbjerg: Power spectrum analysis with least-squares fitting: Amplitude bias and its elimination, with application to optical tweezers and atomic force microscope cantilevers. *Rev. Sci. Instrum.*, 81(7) (2010)

5. K. C. Neuman and S. M. Block: Optical trapping. *Rev. Sci. Instrum.*, 75(9), 2787-2809 (2004)

6. K. Berg-Sorensen and H. Flyvbjerg: Power spectrum analysis for optical tweezers. *Rev. Sci. Instrum.*, 75(3), 594-612 (2004)

7. K. Berg-Sorensen, L. Oddershede, E. L. Florin and H. Flyvbjerg: Unintended filtering in a typical photodiode detection system for optical tweezers. *J. Appl. Phys.*, 93(6), 3167-3176 (2003)

8. D. Klaue and R. Seidel: Torsional Stiffness of Single Superparamagnetic Microspheres in an External Magnetic Field. *Physical Review Letters*, 102(2) (2009)

9. A. Goel, M. D. Frank-Kamenetskii, T. Ellenberger and D. Herschbach: Tuning DNA "strings": Modulating the rate of DNA replication with mechanical tension. *Proc. Natl. Acad. Sci. USA*, 98(15), 8485-8489 (2001)

10. I. Rouzina and V. A. Bloomfield: Force-induced melting of the DNA double helix - 1. Thermodynamic analysis. *Biophys. J.*, 80(2), 882-893 (2001)

11. M. C. Williams, J. R. Wenner, I. Rouzina and V. A. Bloomfield: Entropy and heat capacity of DNA melting from temperature dependence of single molecule stretching. *Biophys. J.*, 80(4), 1932-1939 (2001)

12. H. Y. Zhang and J. F. Marko: Maxwell relations for single-DNA experiments: Monitoring protein binding and double-helix torque with force-extension measurements. *Physical Review E*, 77(3) (2008)

13. O. Otto, F. Czerwinski, J. L. Gornall, G. Stober, L. B. Oddershede, R. Seidel and U. F. Keyser: Real-time particle tracking at 10,000 fps using optical fiber illumination. *Opt. Express*, 18(22), 22722-22733 (2010)

14. C. Danilowicz, D. Greenfield and M. Prentiss: Dissociation of ligand-receptor complexes using magnetic tweezers. *Anal. Chem.*, 77(10), 3023-3028 (2005)

15. K. Kim and O. A. Saleh: A high-resolution magnetic tweezer for single-molecule measurements. *Nucl. Acids Res.*, 37(20), e136 (2009)

16. A. Celedon, I. M. Nodelman, B. Wildt, R. Dewan, P. Searson, D. Wirtz, G. D. Bowman and S. X. Sun: Magnetic Tweezers Measurement of Single Molecule Torque. *Nano Letters*, 9(4), 1720-1725 (2009)

17. J. Lipfert, J. W. J. Kerssemakers, T. Jager and N. H. Dekker: Magnetic torque tweezers: measuring torsional stiffness in DNA and RecA-DNA filaments. *Nat Meth*, 7(12), 977-980 (2010)

18. T. R. Strick, V. Croquette and D. Bensimon: Single-molecule analysis of DNA uncoiling by a type II topoisomerase. *Nature*, 404(6780), 901-904 (2000)

19. O. A. Saleh, S. Bigot, F. X. Barre and J. F. Allemand: Analysis of DNA supercoil induction by FtsK indicates translocation without groove-tracking. *Nat. Struct. Mol. Biol.*, 12(5), 436-440 (2005)

20. R. Seidel, J. van Noort, C. van der Scheer, J. G. P. Bloom, N. H. Dekker, C. F. Dutta, A. Blundell, T. Robinson, K. Firman and C. Dekker: Real-time observation of DNA translocation by the type I restriction modification enzyme EcoR124I. *Nat. Struct. Mol. Biol.*, 11(9), 838-843 (2004)

21. O. A. Saleh, C. Perals, F.-X. Barre and J.-F. Allemand: Fast, DNA-sequence independent translocation by FtsK in a single-molecule experiment. *EMBO J.*, 23(12), 2430-2439 (2004)

22. J. L. Ptacin, M. Nollmann, E. C. Becker, N. R. Cozzarelli, K. Pogliano and C. Bustamante: Sequence-directed DNA export guides chromosome translocation during sporulation in Bacillus subtilis. *Nat. Struct. Mol. Biol.*, 15(5), 485-493 (2008)

23. Y. Harada, O. Ohara, A. Takatsuki, H. Itoh, N. Shimamoto and K. Kinosita: Direct observation of DNA rotation during transcription by Escherichia coli RNA polymerase. *Nature*, 409(6816), 113-115 (2001)

24. A. Revyakin, R. H. Ebright and T. R. Strick: Single-molecule DNA nanomanipulation: improved resolution through use of shorter DNA fragments. *Nature Methods*, 2(2), 127-138 (2005)

25. T. R. Strick, J.-F. Allemand, D. Bensimon and V. Croquette: Behavior of supercoiled DNA. *Biophys. J.*, 74(4), 2016-2028 (1998)

26. N. H. Dekker, V. V. Rybenkov, M. Duguet, N. J. Crisona, N. R. Cozzarelli, D. Bensimon and V. Croquette: The mechanism of type IA topoisomerases. *Proc. Natl. Acad. Sci. U. S. A.*, 99(19), 12126-12131 (2002)

27. N. H. Dekker, V. Rybenkov, M. Duguet, D. Bensimon and V. Croquette: Single molecule studies of prokaryotic topoisomerase I. *Biophys. J.*, 82(1), 507A-507A (2002)

28. G. Charvin, D. Bensimon and V. Croquette: Single-molecule study of DNA unlinking by eukaryotic and prokaryotic type-II topoisomerases. *PNAS*, 100(17), 9820-9825 (2003)

29. G. Charvin, T. R. Strick, D. Bensimon and V. Croquette: Tracking topoisomerase activity at the single-molecule level. *Annu. Rev. Biophys. Biomol. Struct.*, 34, 201-219 (2005)

30. K. C. Neuman, G. Charvin, D. Bensimon and V. Croquette: Mechanisms of chiral discrimination by topoisomerase IV. *Proc. Natl. Acad. Sci. U. S. A.*, 106(17), 6986-6991 (2009)

31. A. Revyakin, C. Y. Liu, R. H. Ebright and T. R. Strick: Abortive initiation and productive initiation by RNA

polymerase involve DNA scrunching. *Science*, 314(5802), 1139-1143 (2006)

32. J.-F. Allemand, D. Bensimon, R. Lavery and V. Croquette: Stretched and overwound DNA forms a Pauling-like structure with exposed bases. *Proc. Natl. Acad. Sci. U. S. A.*, 95(24), 14152-14157 (1998)

33. D. E. Smith, S. J. Tans, S. B. Smith, S. Grimes, D. L. Anderson and C. Bustamante: The bacteriophage phi 29 portal motor can package DNA against a large internal force. *Nature*, 413(6857), 748-752 (2001)

34. H. Yin, M. D. Wang, K. Svoboda, R. Landick, S. M. Block and J. Gelles: Transcription Against an Applied Force. *Science*, 270(5242), 1653-1657 (1995)

35. T. T. Perkins, H. W. Li, R. V. Dalal, J. Gelles and S. M. Block: Forward and reverse motion of single RecBCD molecules on DNA. *Biophys. J.*, 86(3), 1640-1648 (2004)

36. A. Dawid, V. Croquette, M. Grigoriev and F. Heslot: Single-molecule study of RuvAB-mediated Holliday-junction migration. *Proc. Natl. Acad. Sci. USA*, 101(32), 11611-11616 (2004)

37. R. Amit, O. Gileadi and J. Stavans: Direct observation of RuvAB-catalyzed branch migration of single Holliday junctions. *Proc. Natl. Acad. Sci. USA*, 101(32), 11605-11610 (2004)

38. L. Reha-Krantz and H. J.: The dnaB gene product of Escherichia coli. I. Purification, homogeneity, and physical properties. *J Biol Chem*, 253, 4043-50 (1978)

39. W. Bujalowski, M. M. Klonowska and M. J. Jezewska: Oligomeric structure of *Escherichia coli* primary replicative helicase DnaB protein. *J. Biol. Chem.*, 269, 31350-31358 (1994)

40. L. Reha-Krantz and H. J.: The dnaB gene product of Escherichia coli. II. Single stranded DNA-dependent ribonucleoside triphosphatase activity. *J Biol Chem*, 253, 4051-7 (1978)

41. K.-i. Arai, S.-i. Yasuda and A. Kornberg: Mechanism of dnaB protein action: I. Crystallization and properties of dnaB protein, an essential replication protein in Escherichia coli. *J. Biol. Chem.*, 256, 5247-5252 (1981)

42. K.-i. Arai and A. Kornberg: Mechanism of *dnaB* protein action: II. ATP hydrolysis by *dnaB* protein dependent on single- or double-stranded DNA. *J. Biol. Chem.*, 256, 5253-5259 (1981)

43. K.-i. Arai and A. Kornberg: Mechanism of *dnaB* Protein Action: III. Allosteric role of ATP in the alteration of DNA structure by *dnaB* protein in priming replication. *J. Biol. Chem.*, 256, 5260-5266 (1981)

44. K. Arai and A. Kornberg: A general priming system employing only dnaB protein and primase for DNA replication. *Proc Natl Acad Sci U S A.* , 76, 4308-12 (1979)

45. K. Arai and A. Kornberg: Mechanism of dnaB protein action. IV. General priming of DNA replication by dnaB protein and primase compared with RNA polymerase. *J Biol Chem.* , 256, 5267-72 (1981)

46. J. H. LeBowitz and R. McMacken: The *Escherichia coli* dnaB replication protein is a DNA helicase. *J. Biol. Chem.*, 261, 4738-4748 (1986)

47. E. Biswas and S. Biswas: Mechanism of DnaB helicase of Escherichia coli: structural domains involved in ATP hydrolysis, DNA binding, and oligomerization. *Biochemistry.*, 38, 10919-28. (1999)

48. E. Biswas and S. Biswas: Mechanism of DNA binding by the DnaB helicase of Escherichia coli: analysis of the roles of domain gamma in DNA binding. *Biochemistry*, 38, 10929-39 (1999)

49. W. Bujalowski and M. Jezewska: Interactions of Escherichia coli primary replicative helicase DnaB protein with single-stranded DNA. The nucleic acid does not wrap around the protein hexamer. *Biochemistry.*, 34, 8513-9 (1995)

50. S. Biswas and E. Biswas-Fiss: Quantitative analysis of binding of single-stranded DNA by Escherichia coli DnaB helicase and the DnaB x DnaC complex. *Biochemistry.*, 45, 11505-13 (2006)

51. W. Bujalowski and M. J. Jezewwska: Kinetic mechanism of the single-stranded DNA recognition by *Escherichia coli* replicative helicase DnaB protein. Application of the matrix projection operator technique to analyze stopped-flow kinetics. *J. Mol. Biol.*, 295, 831-852 (2000)

52. M. J. Jezewska, S. Rajendran and W. Bujalowski: Complex of *Escherichia coli* primary replicative helicase DnaB protein with a replication fork: recognition and structure. *Biochemistry*, 37, 3116-3136 (1998)

53. W. Bujalowski and M. Jezewska: Kinetic mechanism of nucleotide cofactor binding to Escherichia coli replicative helicase DnaB protein. stopped-flow kinetic studies using fluorescent, ribose-, and base-modified nucleotide analogues. *Biochemistry.*, 39, 2106-22 (2000)

54. S. Rajendran, M. J. Jezewska and W. Bujalowski: Multiple-step kinetic mechanism of DNA-independent ATP binding and hydrolysis by Escherichia coli replicative helicase DnaB protein: quantitative analysis using the rapid quench-flow method. *J. Mol. Biol.*, 303, 773-795 (2000)

55. A. Roychowdhury, M. Szymanski, M. Jezewska and W. Bujalowski: Mechanism of NTP hydrolysis by the Escherichia coli primary replicative helicase DnaB protein. 2. Nucleotide and nucleic acid specificities. *Biochemistry.*, 48, 6730-46 (2009)

56. E. H. Egelman, X. Yu, R. Wild, M. M. Hingorani and S. S. Patel: Bacteriophage T7 helicase/primase proteins form rings around single-stranded DNA that suggest a general structure for hexameric helicases. *Proc. Natl. Acad. Sci. USA*, 92, 3869-3873 (1995)

57. X. Yu, M. M. Hingorani, S. S. Patel and E. H. Egelman: DNA is bound within the central hole to one or two of the six subunits of the T7 DNA helicase. *Nature Struct. Biol.*, 3, 740-743 (1996)

58. S. W. Matson, S. Tabor and C. C. Richardson: The gene 4 protein of bacteriophage T7: Characterization of helicase activity. *J. Biol. Chem.*, 258, 14017-14024 (1983)

59. R. L. Yong Y: Benzo[a]pyrene-DNA adducts inhibit the DNA helicase activity of the bacteriophage T7 gene 4 protein. *Chem Res Toxicol.* , 9, 179-87 (1996)

60. M. J. Jezewska, S. Rajendran, D. Bujalowska and W. Bujalowski: Does single-stranded DNA pass through the inner channel of the protein hexamer in complex with the *Escherichia coli* DnaB helicase? Fluorescence energy transfer studies. *J. Biol. Chem.*, 273, 10515-10529 (1998)

61. R. Galletto, M. J. Jezewska and W. Bujalowski: Unzipping mechanism of the double-stranded DNA unwinding by a hexameric helicase: quantitative analysis of the rate of the dsDNA unwinding, processivity, and kinetic-step-size of the Escherichia coli DnaB helicase using rapid quench-flow method. *J Mol Biol*, 343, 83-99 (2004)

62. R. Galletto, M. Jezewska and W. Bujalowski: Unzipping mechanism of the double-stranded DNA unwinding by a hexameric helicase: the effect of the 3' arm and the stability of the dsDNA on the unwinding activity of the Escherichia coli DnaB helicase. *J Mol Biol.*, 343, 101-14 (2004)

63. M. C. S. Martin, N. P. J. Stamford, N. Dammerova and N. E. Dixon: A structural model for the *Escherichia coli* DnaB helicase based on electron microscopy data. *Journal of Structural Biology*, 114, 167-176 (1995)

64. C. S. Martin, M. Radermacher, B. Wolpensinger, A. Engel, C. S. Miles, N. E. Dixon and J.-m. Carazo: Three-dimensional reconstructions from cryoelectron microscopy images reveal and intimate complex between helicase DnaB and its loading partner DnaC. *Structure*, 6, 501-509 (1998)

65. X. Yu, M. J. Jezewska, W. Bujalowski and E. H. Egelman: The hexameric *E. coli* DnaB helicase can exist in different quaternary states. *J. Mol. Biol.*, 259, 7-14 (1996)

66. S. Yang, X. Yu, M. VanLoock, M. Jezewska, W. Bujalowski and E. Egelman: Flexibility of the rings: structural asymmetry in the DnaB hexameric helicase. *J. Mol. Biol.*, 321, 839-849 (2002)

67. M. R. Sawaya, S. Guo, S. Tabor, C. C. Richardson and T. Ellenberger: Crystal structure of the helicase domain from the replicative helicase-primase of bacteriophage T7. *Cell*, 99, 167-177 (1999)

68. M. R. Singleton, M. R. Sawaya, T. Ellenberger and D. B. Wigley: Crystal structure of T7 gene 4 ring helicase indicates a mechanism for sequential hydrolysis of nucleotides. *Cell*, 101, 589-600 (2000)

69. E. Toth, Y. Li, M. Sawaya, Y. Cheng and T. Ellenberger: The crystal structure of the bifunctional primase-helicase of bacteriophage T7. *Mol Cell*, 12, 1113-23 (2003)

70. D. Fass, C. E. Bogden and J. M. Berger: Crystal structure of the N-terminal domain of the DnaB hexameric helicase. *Structure*, 7, 691-698 (1999)

71. J. Weigelt, S. E. Brown, C. S. Miles, N. E. Dixon and G. Otting: NMR structure of the N-terminal domain of *E. coli* DnaB helicase: implications for structure rearrangements in the helicase hexamer. *Structure*, 7, 681-690 (1999)

72. E. W. Bailey S, Steitz TA.: The crystal structure of the Thermus aquaticus DnaB helicase monomer. *Nucleic Acids Res.*, 35, 4728-36 (2007)

73. S. Bailey, W. Eliason and T. Steitz: Structure of hexameric DnaB helicase and its complex with a domain of DnaG primase. *Science*, 318, 459-63 (2007)

74. G. Wang, M. Klein, E. Tokonzaba, Y. Zhang, L. Holden and X. Chen: The structure of a DnaB-family replicative helicase and its interactions with primase. *Nat Struct Mol Biol.*, 15, 94-100 (2008)

75. D. Kaplan and I. Bruck: Methods to study how replication fork helicases unwind DNA. *Methods Mol Biol.*, 587, 127-35 (2010)

76. A. Yuzhakov, J. Turner and M. O'Donnell: Replisome assembly reveals the basis for asymmetric function in leading and lagging strand replication. *Cell*, 86, 877-886 (1996)

77. D. L. Kaplan and T. A. Steitz: DnaB from *Thermus aquaticus* unwinds forked duplex DNA with an asymmetric tail length dependence. *J. Biol. Chem.*, 274(11), 6889-6897 (1999)

78. D. L. Kaplan: The 3'-tail of a forked-duplex sterically determines whether one or two DNA strands pass through the central channel of a replication-fork helicase. *J. Mol. Biol.*, 301, 285-299 (2000)

79. D. L. Kaplan and M. O'Donnell: DnaB drives DNA branch migration and dislodges proteins while encircling two DNA strands. *Mol. Cell*, 10, 647-657 (2002)

80. D. L. Kaplan and M. O'Donnell: Twin DNA Pumps of a Hexameric Helicase Provide Power to Simultaneously Melt Two Duplexes. *Mol Cell*, 15, 453-465 (2004)

81. S. Kim, H. G. Dallmann, C. S. McHenry and K. J. Marians: Coupling of a replicative polymerase and helicase: a τ-DnaB interaction mediates rapid replication fork movement. *Cell*, 84, 643-650 (1996)

82. M. CS: DNA replicases from a bacterial perspective. *Annu Rev Biochem.*, 80, 403-36 (2011)

83. I. C. Langston LD, O'Donnell M.: Whither the replisome: emerging perspectives on the dynamic nature of the DNA replication machinery. *Cell Cycle*, 8, 2686-91 (2009)

84. M. K. Heller RC: Replisome assembly and the direct restart of stalled replication forks. *Nat Rev Mol Cell Biol.* , 7, 932-43 (2006)

85. Y.-B. Lu, V. A. L. R. Pillarisetty, B. K. Mohanty and D. Bastia: Direct physical interaction between DnaG primase and DnaB helicase of *Escherichia coli* is necessary for optimal synthesis of primer RNA. *Proc. Natl. Acad. Sci. USA*, 93, 12902-12907 (1996)

86. K. Tougu and K. J. Marians: The interaction between helicase and primase sets the replication fork clock. *J. Biol. Chem.*, 271, 21398-21405 (1996)

87. A. Mitkova, S. Khopde and S. Biswas: Mechanism and stoichiometry of interaction of DnaG primase with DnaB helicase of Escherichia coli in RNA primer synthesis. *J Biol Chem*, 278, 52253-61 (2003)

88. M. J. Davey, L. Fang, P. McInerney, R. E. Georgescu and M. O'Donnell: The DnaC helicase loader is a dual ATP/ADP switch protein. *EMBO J.*, 21, 3148-3159 (2002)

89. M. Makowska-Grzyska and J. Kaguni: Primase directs the release of DnaC from DnaB. *Mol Cell*, 37, 90-101 (2010)

90. J. Kaguni: Replication initiation at the Escherichia coli chromosomal origin. *Curr Opin Chem Biol.*, [Epub ahead of print] (2011)

91. A. Roychowdhury, M. Szymanski, M. Jezewska and W. Bujalowski Interactions of the Escherichia coli DnaB-DnaC protein complex with nucleotide cofactors. 1. Allosteric conformational transitions of the complex. *Biochemistry*, 2009, 6712-29 (2009)

92. A. Roychowdhury, M. Szymanski, M. Jezewska and W. Bujalowski: Escherichia coli DnaB helicase-DnaC protein complex: allosteric effects of the nucleotides on the nucleic acid binding and the kinetic mechanism of NTP hydrolysis. 3. *Biochemistry*, 48, 6747-63 (2009)

93. K. Carr and J. Kaguni: Escherichia coli DnaA protein loads a single DnaB helicase at a DnaA box hairpin. *J Biol Chem*, 277, 39815-22 (2002)

94. B. Learn, S. Um, L. Huang and R. McMacken: Cryptic single-stranded-DNA binding activities of the phage lambda P and Escherichia coli DnaC replication initiation proteins facilitate the transfer of E. coli DnaB helicase onto DNA. *Proc Natl Acad Sci U S A.*, 94, 1154-9 (1997)

95. M. Gupta, J. Atkinson and P. McGlynn: DNA structure specificity conferred on a replicative helicase by its loader. *J Biol Chem.*, 285, 979-87 (2010)

96. R. Heller and K. Marians: Replisome assembly and the direct restart of stalled replication forks. *Nat Rev Mol Cell Biol.* , 7, 932-43 (2006)

97. C. Gabbai and K. Marians: Recruitment to stalled replication forks of the PriA DNA helicase and replisome-loading activities is essential for survival. *DNA Repair (Amst).* , 9, 202-9 (2010)

98. J. Atkinson, M. Gupta and P. McGlynn: Interaction of Rep and DnaB on DNA. *Nucleic Acids Res.*, 39, 1351-9 (2011)

99. J. Atkinson, M. Gupta, C. Rudolph, H. Bell, R. Lloyd and P. McGlynn: Localization of an accessory helicase at the replisome is critical in sustaining efficient genome duplication. *Nucleic Acids Res.*, 39, 949-57 (2011)

100. B. D. Kaplan DL: Mechanisms of polar arrest of a replication fork. *Mol Microbiol.* , 72, 279-85 (2009)

101. M. D. Mulcair, P. M. Schaeffer, A. J. Oakley, H. F. Cross, C. Neylon, T. M. Hill and N. E. Dixon: A Molecular Mousetrap Determines Polarity of Termination of DNA Replication in *E. coli*. *Cell*, 125, 1309-1313 (2006)

102. D. Bastia and B. Mohanty: Termination of DNA Replication. In: *DNA replication and human disease.* Ed M. DePamphilis. Cold Spring Harbor Laboratory Press, Cold Spring Harbor, NY (2006)

103. C. Neylon, A. V. Kralicek, T. M. Hill and N. E. Dixon: Replication Termination in *Escherichia coli*: Structure and Antihelicase Activity of the Tus-*Ter* Complex. *Microbiol Mol Biol Rev*, 69, 1092-2172 (2005)

104. C. Indiani, L. Langston, O. Yurieva, M. Goodman and M. O'Donnell: Translesion DNA polymerases remodel the replisome and alter the speed of the replicative helicase. *Proc Natl Acad Sci U S A*, 106, 6031-8 (2009)

105. N. Ribeck, D. L. Kaplan, I. Bruck and O. A. Saleh: DnaB helicase activity is modulated by DNA geometry and force. *Biophys. J.*, 99(7), 2170-2179 (2010)

106. T. Lionnet, M. M. Spiering, S. J. Benkovic, D. Bensimon and V. Croquette: Real-time observation of bacteriophage T4 gp41 helicase reveals an unwinding mechanism. *Proc. Natl. Acad. Sci. USA*, 104(50), 19790-19795 (2007)

107. J. D. Wen, L. Lancaster, C. Hodges, A. C. Zeri, S. H. Yoshimura, H. F. Noller, C. Bustamante and I. Tinoco: Following translation by single ribosomes one codon at a time. *Nature*, 452(7187), 598-U2 (2008)

108. T. Lionnet, A. Dawid, S. Bigot, F. X. Barre, O. A. Saleh, F. Heslot, J. F. Allemand, D. Bensimon and V. Croquette: DNA mechanics as a tool to probe helicase and translocase activity. *Nucleic Acids Res.*, 34(15), 4232-4244 (2006)

109. W. Cheng, S. Dumont, I. Tinoco and C. Bustamante: NS3 helicase actively separates RNA strands and senses sequence barriers ahead of the opening fork. *Proc. Natl. Acad. Sci. USA*, 104(35), 13954-13959 (2007)

110. M. Manosas, M. M. Spiering, Z. Zhuang, S. J. Benkovic and V. Croquette: Coupling DNA unwinding activity with primer synthesis in the bacteriophage T4 primosome. *Nat Chem Biol*, 5(12), 904-912 (2009)

111. S. Dumont, W. Cheng, V. Serebrov, R. K. Beran, I. Tinoco, A. M. Pyle and C. Bustamante: RNA translocation and unwinding mechanism of HCV NS3 helicase and its coordination by ATP. *Nature*, 439(7072), 105-108 (2006)

112. J. F. Marko and E. D. Siggia: Stretching DNA. *Macromolecules*, 28(26), 8759-8770 (1995)

113. D. B. McIntosh and O. A. Saleh: Salt Species-Dependent Electrostatic Effects on ssDNA Elasticity. *Macromolecules*, 44(7), 2328-2333 (2011)

114. O. A. Saleh, D. B. McIntosh, P. Pincus and N. Ribeck: Nonlinear Low-Force Elasticity of Single-Stranded DNA Molecules. *Physical Review Letters*, 102(6), 068301-4 (2009)

115. G. J. L. Wuite, S. B. Smith, M. Young, D. Keller and C. Bustamante: Single-molecule studies of the effect of template tension on T7 DNA polymerase activity. *Nature*, 404(6773), 103-106 (2000)

116. B. Maier, D. Bensimon and V. Croquette: Replication by a single DNA polymerase of a stretched single-stranded DNA. *Proc. Natl. Acad. Sci. U. S. A.*, 97(22), 12002-12007 (2000)

117. M. N. Dessinges, T. Lionnet, X. G. Xi, D. Bensimon and V. Croquette: Single-molecule assay reveals strand switching and enhanced processivity of UvrD. *Proc. Natl. Acad. Sci. U. S. A.*, 101(17), 6439-6444 (2004)

118. N. A. Tanner, S. M. Hamdan, S. Jergic, P. M. Schaeffer, N. E. Dixon and A. M. van Oijen: Single-molecule studies of fork dynamics in *Escherichia coli* DNA replication. *Nat. Struct. Mol. Biol.*, 15(2), 170-176 (2008)

119. C. Bustamante, Y. R. Chemla, N. R. Forde and D. Izhaky: Mechanical processes in biochemistry. *Annu. Rev. Biochem.*, 73, 705-748 (2004)

120. T. M. Lohman: Escherichia coli DNA helicases: mechanisms of DNA unwinding. *Mol. Microbiol.*, 6(1), 5-14 (1992)

121. M. Manosas, X. G. Xi, D. Bensimon and V. Croquette: Active and passive mechanisms of helicases. *Nucleic Acids Res.*, 38(16), 5518-5526 (2010)

122. M. D. Betterton and F. Julicher: Opening of nucleic-acid double strands by helicases: Active versus passive opening. *Phys. Rev. E*, 71(1), 011904 (2005)

123. M. D. Betterton and F. Julicher: A motor that makes its own track: Helicase unwinding of DNA. *Phys. Rev. Lett.*, 91(25), 258103 (2003)

124. D. S. Johnson, L. Bai, B. Y. Smith, S. S. Patel and M. D. Wang: Single-molecule studies reveal dynamics of DNA unwinding by the ring-shaped T7 helicase. *Cell*, 129(7), 1299-1309 (2007)

125. R. Galletto, M. J. Jezewska and W. Bujalowski: Unzipping mechanism of the double-stranded DNA unwinding by a hexameric helicase: The effect of the 3' arm and the stability of the dsDNA on the unwinding activity of the *Escherichia coli* DnaB helicase. *J. Mol. Biol.*, 343(1), 101-114 (2004)

126. I. Bonnet, A. Biebricher, P.-L. Porté, C. Loverdo, O. Bénichou, R. Voituriez, C. Escudé, W. Wende, A. Pingoud and P. Desbiolles: Sliding and jumping of single EcoRV restriction enzymes on non-cognate DNA. *Nucleic Acids Res.*, 36(12), 4118-4127 (2008)

127. J. van Mameren, M. Modesti, R. Kanaar, C. Wyman, E. J. G. Peterman and G. J. L. Wuite: Counting RAD51 proteins disassembling from nucleoprotein filaments under tension. *Nature*, 457(7230), 745-748 (2009)

Abbreviations: SMM: Single-molecule manipulation, ssDNA: single-stranded DNA**,** dsDNA: double-stranded DNA. MT: magnetic tweezers

Key Words: Motor proteins, Helicases, DnaB, Single-Molecule, Branch-Migration, Review

Send correspondence to: Daniel L. Kaplan, Vanderbilt University, VU Station B, Box 35-1634, Department of Biological Sciences, Nashville, TN 37235, Tel: 615-322-2072, Fax: 615-343-6707, E-mail: Daniel.Kaplan@Vanderbilt.Edu